




VI-RADS for Bladder Cancer: Current Applications and Future Developments

Valeria Panebianco, MD,^{1†*}  Martina Pecoraro, MD,¹ Francesco Del Giudice, MD,² Mitsuru Takeuchi, PhD,³ Valdair F. Muglia, PhD,⁴  Emanuele Messina, MD,¹ Stefano Cipollari, MD,¹ Gianluca Giannarini, MD,⁵  Carlo Catalano, MD,¹ and Yoshifumi Narumi, PhD^{6†}

Bladder cancer (BCa) is among the ten most frequent cancers globally. It is the tumor with the highest lifetime treatment-associated costs, and among the tumors with the heaviest impacts on postoperative quality of life. The purpose of this article is to review the current applications and future perspectives of the Vesical Imaging Reporting and Data System (VI-RADS). VI-RADS is a newly developed scoring system aimed at standardization of MRI acquisition, interpretation, and reporting for BCa. An insight will be given on the BCa natural history, current MRI applications for local BCa staging with assessment of muscle invasiveness, and clinical implications of the score for disease management. Future applications include risk stratification of nonmuscle invasive BCa, surveillance, and prediction and monitoring of therapy response.

Level of Evidence: 3

Technical Efficacy Stage: 2

J. MAGN. RESON. IMAGING 2020.

BLADDER CANCER (BCa) is among the ten most frequent cancers globally.¹ Every year ~550,000 people are diagnosed with bladder cancer.² Major risk factors for the development are cigarette smoking, with a population-attributable risk of BC of about 40%,³ and other environmental factors such as exposure to chemicals and industrial pollutants.

The initial diagnostic workup for BCa involves ultrasound (US) or cystoscopy as first-line tests, followed by diagnostic transurethral resection of bladder tumor (TURBT) for the confirmatory pathology. Around 70% of tumors are nonmuscle-invasive bladder cancer (NMIBC), and more than 50% are Ta stage tumors.^{1,4} Although the majority of cases are diagnosed at a nonmuscle-invasive stage, ~200,000 deaths occur each year due to BCa.⁵ The rate of progression and recurrence of the disease is high; nearly three-fourths of patients diagnosed with high-risk BCa will recur, progress, or die within 10 years from their diagnosis, partly due to the

inaccuracies of the diagnostic procedure.⁶ Epidemiological studies show that between 30% and 45% of deaths are preventable.⁷

Mortality among different countries is heterogeneous, with the highest rates observed in countries such as the Middle East and North Africa.⁸ There is a significant relation between BCa mortality and the world development index, strengthening the hypothesis that a higher degree of socioeconomic development is able to provide earlier diagnosis and more appropriate treatment. BCa survival is strongly dependent on the treatment delivered, rather than the intrinsic aggressiveness of the tumor.⁹ High rates of inaccuracy are not only responsible for the increased morbidity and mortality, but they also translate into higher costs. With the current diagnostic protocol, the risk of residual disease after initial TURBT may be as high as 50–70%, with the need to perform an additional tumor resection (re-TURBT) for restaging the tumor.¹⁰ This constitutes a significant preventable

View this article online at wileyonlinelibrary.com. DOI: 10.1002/jmri.27361

Received Apr 16, 2020, Accepted for publication Aug 27, 2020.

*Address reprint requests to: V.P., Viale del Policlinico 155, 00161 Rome, Italy. E-mail: valeria.panebianco@uniroma1.it

[†]These authors contributed equally.

From the ¹Department of Radiological Sciences, Oncology and Pathology, Sapienza/Policlinico Umberto I, Rome, Italy; ²Department of Maternal-Infant and Urological Sciences, Sapienza/Policlinico Umberto I, Rome, Italy; ³Department of Radiology, Radiolonet Tokai, Nagoya, Japan; ⁴Department of Medical Images, Radiation Therapy and Oncohematology, Ribeirao Preto Medical School, University of Sao Paulo, Ribeirao Preto, Brazil; ⁵Urology Unit, Academic Medical Centre "Santa Maria della Misericordia", Udine, Italy; and ⁶Department of Healthcare, Tachibana University, Kyoto, Japan

expense, considering the additional surgical procedure and hospital admissions that it requires. It is not a surprise that BCa is currently the tumor with the highest lifetime treatment-associated costs, with around \$185,000 expenditure per case, and around \$4 billion national costs of cancer care in the U.S. per year.^{11,12} Despite the advancements in surgical and pharmacologic treatment, the primary diagnostic and therapeutic planning still need to be improved: BCa is currently among the tumors with the heaviest impacts on postoperative quality of life.^{13–15} An implementation of the accuracy of the primary staging of the tumor is of vital importance at the present time, for different pathologies.^{16–19}

In order to optimize the diagnostic pathway and minimize costs related to BCa management, new diagnostic techniques are being proposed. Preoperative multiparametric magnetic resonance imaging (MRI), with the use of the Vesical Imaging Reporting and Data System (VI-RADS) scoring system seems to constitute a possible solution to this issue.

Bladder Anatomy and Bladder Cancer

The bladder is a hollow pelvic organ, connected to the ureters and to the urethra. As part of the urinary system, it is devoted to the collection of urine: it can accommodate 400–600 mL of urine (full distension), owing to the unique properties of its anatomy. The urothelium is a pseudostratified columnar epithelium composed of three cell types—the apical umbrella, the medial, and the basal cells—highly modifiable in shape.²⁰ The pseudostratified epithelium can display up to seven layers of cells, sliding one or the other over a single basement membrane. Underlying the mucosa, the lamina propria is found, a highly vascularized layer of connective tissue. The outer layer is the muscularis propria (made of three well-represented layers of smooth muscle tissue: an inner longitudinal, a middle circular, and an outer longitudinal). The outermost layer is the adventitia: mesenchymal tissue that envelops the bladder and makes contact with the nearby infraperitoneal organs.²¹ Thanks to the characteristics of its tissues, the bladder can display outstanding distensible properties and contractile strength at the same time.

The most frequent histologic variant of BCa is urothelial cell carcinoma, accounting for more than 90% of all cases; other lesser variants are squamous cell carcinoma, adenocarcinomas, and lymphomas.²² Urothelial carcinoma is an epithelial tumor arising from transitional cells of the bladder mucosa. It typically displays multifocal and a recurrent nature.^{23,24} The morphology of the tumor is variable, and the different variants can sometimes constitute a continuum in the evolution of the neoplasm. The primary tumor can form exophytic polypoid masses, or sessile infiltrative lesions; carcinoma-in-situ (CIS) instead has a horizontal, highly invasive growth. Invasion of the muscularis propria (pT2) is a key predictive and prognostic factor: there is a considerable drop

in prognosis from nonmuscle-invasive and muscle-invasive BCa.²⁵ For this reason, the pathologic and radiologic assessment of muscle invasion is of fundamental importance, and affects therapeutic planning dramatically.²⁶

Bladder Cancer Staging and MRI

The TNM system is used to stage BCa.²⁷ T_a tumor infiltrates the innermost layer of the bladder lining. T₁ cancer grows into the connective tissue, not invading the detrusor muscle layer. T₂ cancer has grown into the muscle, with T_{2a} into the superficial and T_{2b} into the deeper lining. T₃ cancer has grown into the adipose tissue layer, with T_{3a} and T_{3b} representing microscopic and macroscopic invasion, respectively. T₄ cancer spreads outside the bladder, with T_{4a} to adjacent organs and T_{4b} to distant tissues, outside pelvis and abdomen. Therefore, BCa staged \leq T₁ is defined as NMIBC and \geq T_{2a} as MIBC, the two having very different prognosis and therapeutic planning. It is essential to accurately differentiate NMIBC and MIBC, since the two require very distinct management. In the setting of BCa staging, MRI of the urinary bladder has proven to be able to accurately differentiate NMIBC from MIBC. MRI strengths lie in its high spatial resolution and soft-tissue contrast.^{28–30}

Local staging is performed, evaluating the presence of muscle-invasiveness (T₁ vs. T₂ stage), perivesical fat invasion (T₃ stage), adjacent structure involvement (T₄ stage), and assessment of pelvic lymph nodes (N stage), and bones (M stage). MRI can properly assess local staging thanks to morphological T₂-weighted images (T₂WI) associated with functional diffusion-weighted images (DWI) / apparent diffusion coefficient (ADC map), and dynamic contrast-enhanced MRI (DCE) sequences. T₂WI allows the evaluation of the location, size, and morphology of bladder lesions, and reduces staging errors thanks to its high signal-to-noise ratio (SNR) and excellent anatomical visualization.³¹ MRI functional sequences application has further increased the accuracy of the technique.^{32–34} On T₂WI, BCa usually has a signal intensity (SI) intermediate to urine and muscle. The detrusor muscle has a low SI on T₂WI, and if discontinuous should raise suspicion of T₂ stage tumor.^{35–37} On DWI, BCa is typically hyperintense (with correspondingly low ADC values), the normal muscle layer is of intermediate SI.^{38,39} In 2009, Takeuchi et al³³ described the inchworm sign recognized in stalked exophytic tumors, representing the arch-shaped hyperintense appearance of the tumor over the hypointense submucosal stalk. They proposed the sign, indicative of a pT₁ or lower tumor, as an imaging biomarker to predict tumor aggressiveness. On DCE MRI, tumors show early enhancement after contrast injection, with the detrusor muscle generally showing late enhancement; muscle-invasiveness (T₂ stage) is suspected whenever the detrusor muscle shows early enhancement.^{35,38,40,41} MRI cannot identify CIS.⁴²

Differentiation between T2a and T2b is defined due to the prognostic significance, with T2b patients carrying a significantly increased risk for lymph node metastasis (14% vs. 30%, respectively) and decreased survival rates⁴³; T2 sub-staging is not feasible with MRI; however, patient management does not change in these two categories.⁴² T3a categorization is not feasible with MRI, and it can only be assigned on pathology specimens.⁴⁴ Again, the management for both T2 and T3a is the same.^{45,46} Fat tissue macroscopic involvement (T3b) is assessed with MRI, with the tumor extending to the perivesical adipose tissue on both T₂WI and DW images, associated with irregularity of the bladder wall and postcontrast enhancement.^{31,46} Whenever there is disruption of the normal SI and morphology of adjacent organs on T₂WI and the DWI/ADC map with associated early enhancement, direct extension of the tumor into the adjacent organ should be suspected and staged as T4 tumor.^{31,47} In 2015, Gandhi et al⁴⁸ published results of a meta-analysis carried out on about 5000 patients, showing that MRI should be considered as potentially superior to the current standard for clinical staging for $\leq T1$ vs. $\geq T2$, $\leq T2$ vs. $\geq T3$, and $< T4b$ vs. $pT4b$, not for T -any vs. $T0$. In 2017, a meta-analysis by Woo et al⁴⁹ showed a pooled sensitivity and specificity of 0.92 and 0.87, respectively, for differentiating stage T1 tumors from T2 or higher. In 2018, in a similar research Huang et al⁵⁰ showed a pooled sensitivity and specificity of 0.90 and 0.88, respectively, with results going up to 0.92 and 0.96 when MRI was performed with a 3T scan, with DWI as part of the acquisition protocol. In 2019, Zhang et al⁵¹ published a meta-analysis on the diagnostic accuracy of MRI as a staging tool for BCa with a total of 140 studies included, showing a pooled sensitivity of 0.84 (95% confidence interval [CI] = 0.79–0.89), specificity of 0.91 (95% CI: = 0.87–0.93), and an area under the curve (AUC) of 0.946.

VI-RADS

In 2018, a panel of multidisciplinary experts developed, through consensus using existing literature, the VI-RADS to standardize MRI acquisition and interpretation for BCa.⁴²

The Protocol

PATIENT PREPARATION. Based on the VI-RADS document, antispasmodic agents could be administered so as to minimize motion and susceptibility artifacts from bowel peristalsis, thus improving imaging acquisition. The application of saturation bands on the anterior abdominal wall can reduce respiratory influences.

Adequate distension of the bladder is vital to avoid false positives and negatives due to up- and understaging. Patients are instructed to void 1–2 hours before imaging and to drink 500–1000 mL of water in the 30 minutes before the examination, depending on individual tolerance. MRI can be used

as real-time imaging to determine bladder filling. Patients with an underdistended bladder should repeat the scan after 30–60 minutes; those with an overdistended bladder should void and start drinking again.⁴² The optimal bladder volume for imaging is around 300 mL; therefore, in patients with a urethral catheter, 250–400 mL sterile saline can be used to distend the bladder.³¹

MRI ACQUISITION PROTOCOL. The minimal acquisition protocol consists of a combination of high-resolution T₂WI on three planes (axial, coronal, and sagittal), and two functional MRI techniques: DWI and DCE MRI. A T₁-weighted (T₁W) image is used to detect the presence of blood products and clot in the bladder, and bone metastasis. All the sequences should display the whole bladder, proximal urethra, pelvic nodes and pelvic viscera (prostate, seminal vesicles, uterus, ovaries, fallopian tubes, and vagina). The use of a high-field scan (1.5 or 3.0T) is recommended to achieve appropriate spatial resolution and SNR. A multichannel phased array body surface coil with at least 16 channels is also recommended.¹⁶ An overview of setting recommendations is presented in Table 1.

T₂-Weighted Images. T₂WI shows the bladder anatomy and is used for tumor detection, localization, evaluation of the size, and morphology. 2D or 3D, fast-spin-echo (FSE) or turbo-spin-echo sequences are acquired with a slice thickness of 3–4 mm and a small field of view (FOV), to achieve appropriate spatial resolution with an acceptable SNR. Images acquired with isotropic voxels can be reformatted using a plane perpendicular to the tumor base.^{52,53}

Diffusion-Weighted Images. DWI reflects the Brownian motion of water molecules and it is a key component of the bladder MRI examination. An axial breathing-free spin-echo EPI sequence with spectral fat saturation is recommended. Acquisition of DW images on the coronal and/or sagittal plane can be performed, especially when tumors are localized at the bladder dome. A DWI sequence consists of multiple b values; typically b 800–1000 s/mm² are required; a very high b value may degrade SNR.^{33,54} Anatomical location is a limit of DWI, and it requires matching with the T₂W images. To minimize mismatch, it is important to have a homogenous magnetic field.⁴⁶ DWI is sensitive to artifacts caused by field inhomogeneities. To reduce artifacts, to achieve a more homogenous field, and to minimize bowel movement, a short echo time (TE) can be used and a small shim box can be applied around the bladder.⁵⁵ Recently, Warndahl et al⁵⁶ proposed a new DWI sequence for the detection of prostate cancer, that could be applied to the bladder. It is acquired with a 2D spatially selective, echo-planar RF pulse to excite a limited extent in the phase FOV direction, showing lower

TABLE 1. Summary Table With MRI Settings at Both 1.5T and 3T Scanner

MRI parameter setting at	T ₂ W		DWI		DCE MRI	
	1.5T	3.0T	1.5T	3.0T	1.5T	3.0T
TR (msec)	5000	4690	4500	2500 up to 5300	3.3	3.8
TE (msec)	80	119	88	61	1.2	1.2
Flip angle (degree)	90	90	90	90	13	15
FOV (cm)	23	23	27	32	35	27
Matrix	256 × 189–256	400 × 256–320	128 × 109	128 × 128	256 × 214	192 × 192
Slice thickness (mm)	4	3–4	4	3–4	2	1
Slice gap (mm)	0–0.4	0–0.4	0–0.4	0.3–0.4	0	0
Number of excitations	1–2	2–3	10–15	4–10	1	1
b value			0–800–1000	0–800–1000 (up to) 2000 s/mm ²		

DCE = dynamic contrast enhancement; DWI = diffusion-weighted imaging; FOV = field of view; MRI = magnetic resonance imaging; TE = echo time; TR = repetition time; T₂WI = T₂ weighted imaging.

susceptibility to field inhomogeneity and significant improvement in interreader agreement and image quality.

Dynamic Contrast-Enhanced MRI. DCE MRI is the final key component of the VI-RADS and bladder MRI acquisition protocol. It reflects tissue vascularity and microvessel permeability. An axial 3D T₁ gradient echo (GRE) sequence with fat suppression is the preferred sequence, allowing higher spatial resolution. When acquired in 3D, images can be reformatted on different planes, which should be perpendicular to the tumor base.

Images are acquired in the precontrast phase and during injection of a gadolinium-based contrast agent. It is administered using an injector system (0.1 mmol/kg of body weight) at a rate of 1.5–2.0 mL/s if a standard relaxivity agent is used and followed by a saline flush. A high temporal resolution of <15 seconds is used to show early enhancement of the tumor. Signal contrast in the inner layer and the muscularis layer decreases with time; therefore, it is not useful to acquire late-phase images for T staging.⁴²

The original VI-RADS document specifies the technical requirements and the acquisition protocol of MRI of the bladder.⁴²

Semeiotics and Reporting

MRI spatial resolution allows to differentiate the bladder “inner layer” (mucosa and lamina propria) from the “outer layer” (muscularis propria) and from the perivesical fat tissue. Specifically, in healthy tissue the “inner layer” is not

visualized on either T₂W or DW images; instead, the detrusor muscle appears as a low SI line on T₂W images, and as an intermediate SI line on DWI and ADC, where urine appears hypo- and hyperintense, respectively. On DCE, the “inner layer” shows early enhancement (hyperintense line); instead, the outer layer shows a more delayed and progressive enhancement. When muscle invasiveness is present, the outer layer immediately below the bladder tumor enhances well.

Diffuse or focal thickening of the bladder wall may appear because of an evolving inflammatory process and/or as a consequence of prior tumor resection, involving the “inner layer” (mucosa and lamina propria). In such cases, a thickened high SI line can be seen on T₂W images representing the edematous inner layer overlaying the low SI muscular layer; on DWI the edematous mucosa is seen as a relatively hypointense line.^{37–39}

Tumor morphology should be assessed on T₂W images. BCa can take several forms: it can be sessile or papillary, and it can show an endo- or exophytic growth pattern; they can also be flat or mixed. Papillary tumors can be broad-based or pedunculated. Pedunculated papillary tumors show a better prognosis than the rest of the BCa forms.³⁸

The most common location of tumor growth is the lateral walls and the bladder base. Few authors have correlated the location of the tumor with a more severe prognosis, with bladder tumor arising from the bladder neck having the worst prognostic significance.^{57,58} The VI-RADS document recommends the use of a schematic bladder map, to further standardize reporting. The presence of multiple tumors should be

recorded, specifying the number of lesions, the size of the largest tumor, and the tumor with the more advanced appearance (highest suspected stage).⁴²

The Score

VI-RADS is a 5-point category scale for MRI of the bladder that allows the radiologist to assign a numerical category to bladder lesions that defines the risk of muscle invasiveness. The score comprises five categories, from 1 to 5, with VI-RADS 1 and 2 representing very low and low likelihood of muscle invasiveness (Fig. 1); VI-RADS 3 reflecting an equivocal category (Fig. 2); VI-RADS 4 and 5, a high and very high likelihood of muscle invasiveness (Figs. 3, 4). In order to minimize the number of false-negative results that would dramatically change the prognostic outcome, VI-RADS ≥ 3 has been suggested as muscle-invasive bladder cancer; however, VI-RADS ≥ 4 is also potentially useful.

The goal of the VI-RADS is to standardize and optimize the image acquisition of MRI of the bladder and to standardize reporting, focused on accurate and reproducible local staging of BCa. It is meant to be applied to untreated patients and to patients having received diagnostic TURBT, before re-TURBT.⁴²

According to VI-RADS, BCa on MRI is defined as an intravesical lesion with T₂ signal intensity intermediate to urine and muscle, a high signal intensity on DWI, matching to a low signal intensity at the ADC map, with early enhancement at DCE-MRI.

Tumors should be assessed on T₂W images, DWI, and DCE singularly, to create an overall risk of the invasion score. The VI-RADS algorithm for overall score assessment sees T₂W images as the “first-pass” sequence for BCa staging for a VI-RADS score from 1 to 3, and DWI (first) and DCE (second; especially if the DWI is suboptimal in quality) as the dominant sequences for risk estimates of scores 4 and 5.⁴² A summary of the pathological staging correlation with the final VI-RADS score according to single categories is depicted in Table 2.

ASSESSMENT ON T₂WI . The single assessment on T₂W images defines the structural category (SC). Interruption of the low SI line representing the muscularis propria, on T₂W images, should raise suspicion of muscle-invasive bladder cancer ($\geq T_2$ stage). SC 1 and 2 is assigned to lesions associated with an uninterrupted low SI line representing the integrity of muscularis propria, smaller or larger than 1 cm,

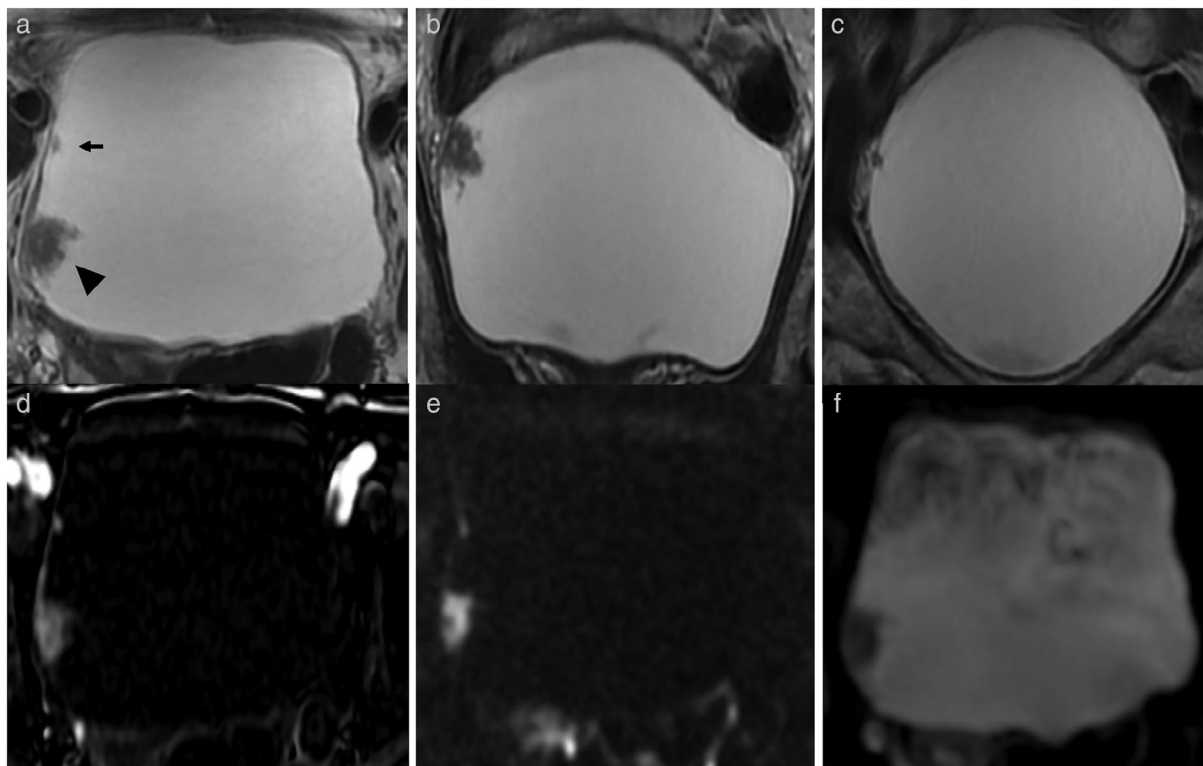


FIGURE 1: A 64-year-old female with positive cystoscopy. (a–c) T₂W imaging (axial, coronal plane) shows two pedunculated masses, one <1 cm in size (arrow) and one >1 cm in size (arrowhead), both in the right lateral bladder wall, the smaller localized more anteriorly, both with intermediate SI not extending through the muscularis propria. T₂W imaging assigned as VIRADS categories 1 and 2, respectively. (d) DCE imaging shows early and heterogeneous enhancement of the lesions, not extending through the muscularis propria; enhancement of the inner layer can be appreciated. DCE assigned as VI-RADS categories 1 and 2, respectively. (e,f) DWI (b = 2000) and ADC maps show significant restricted diffusion, not extending through the muscularis propria; the inchworm sign can be appreciated at the posterior lesion. DWI assigned as VIRADS categories 2 and 1, respectively. Overall VI-RADS score was 1 for the smaller mass and 2 for the larger.

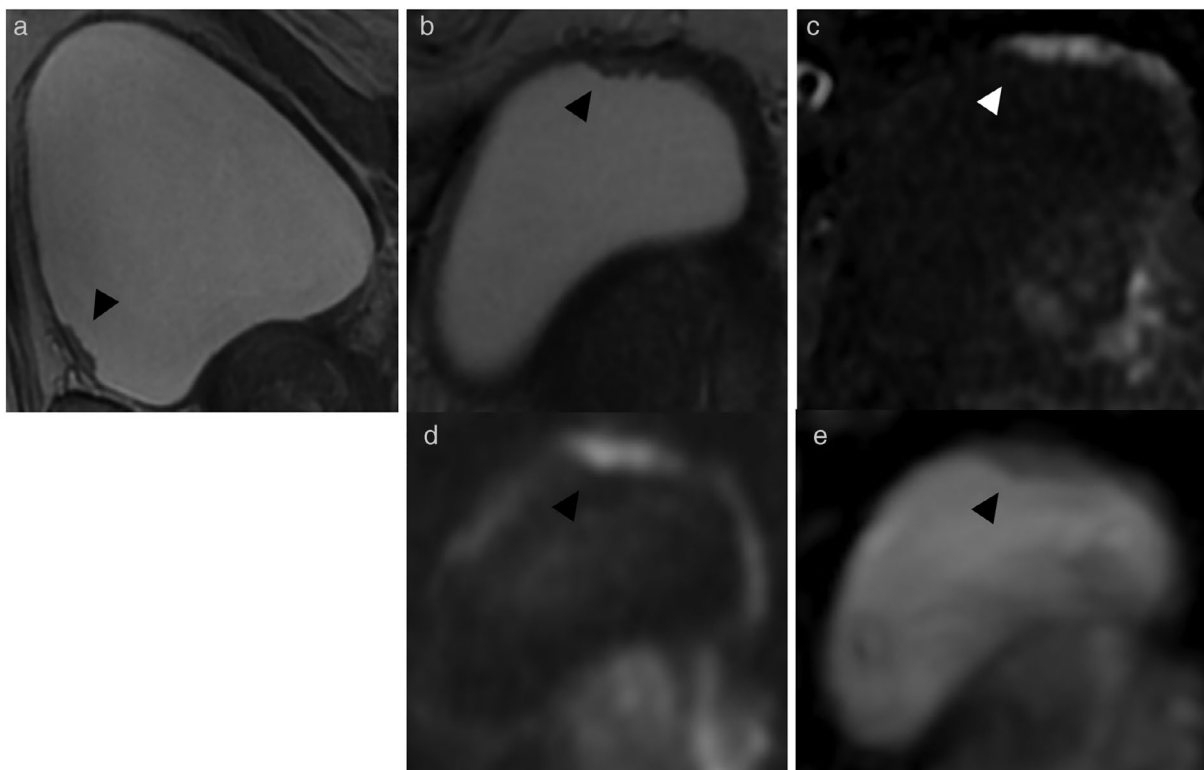


FIGURE 2: A 75-year-old male treated with TURB for NMIBC. (a,b) T₂W imaging (sagittal, axial plane) shows a sessile mass >1 cm in size (arrowhead) at the level of the anterior bladder wall, with intermediate SI that does not extend through the muscularis propria. T₂W imaging assigned as VIRADS category 2. (c) DCE imaging shows early and heterogeneous enhancement of the lesion, not clearly extending through the muscularis propria. DCE assigned as VI-RADS category 3. (d,e) DWI (b = 2000) and ADC maps show a lesion with significant restricted diffusion, not clearly extending through the muscularis propria. DWI assigned as VIRADS category 3. Overall VI-RADS score was 3.

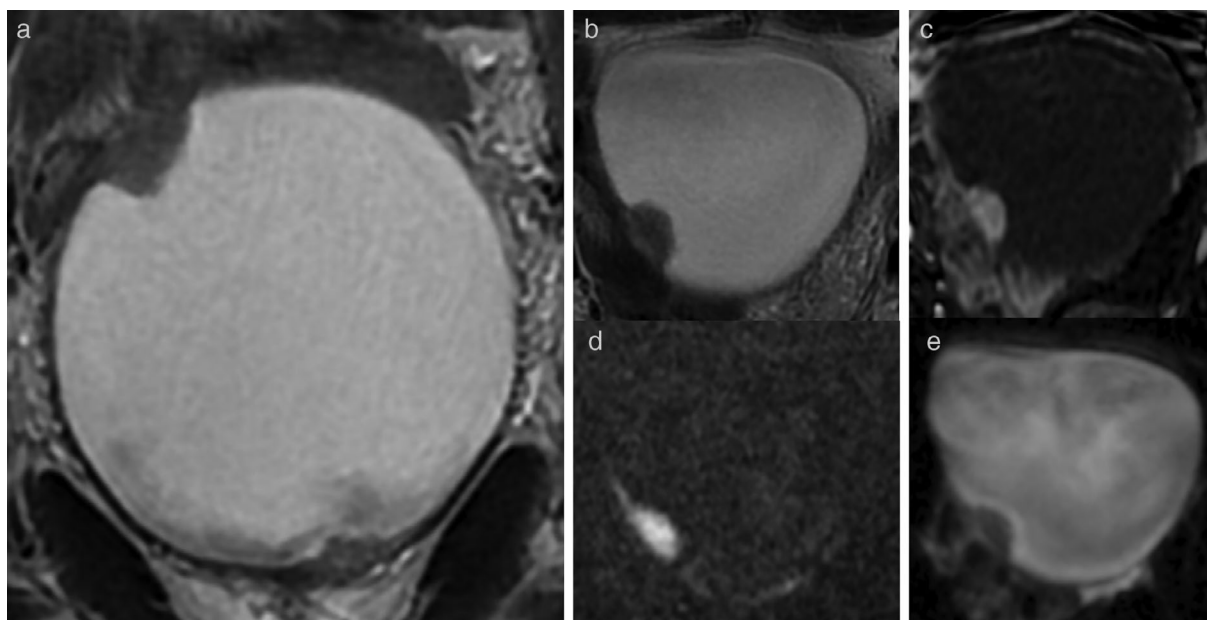


FIGURE 3: A 72-year-old male with positive cystoscopy. (a,b) T₂W imaging (coronal, axial plane) shows a sessile mass >1 cm in size at the level of the right lateral bladder wall/dome of the bladder, with intermediate SI that extends through the muscularis propria. T₂W imaging assigned as VIRADS category 4. (c) DCE imaging shows early and heterogeneous enhancement of the lesion, extending through the muscularis propria. DCE assigned as VI-RADS category 4. (d,e) DWI (b = 2000) and ADC maps show a lesion with significant restricted diffusion, extending through the muscularis propria. DWI assigned as VIRADS category 4. Overall VI-RADS score was 4.

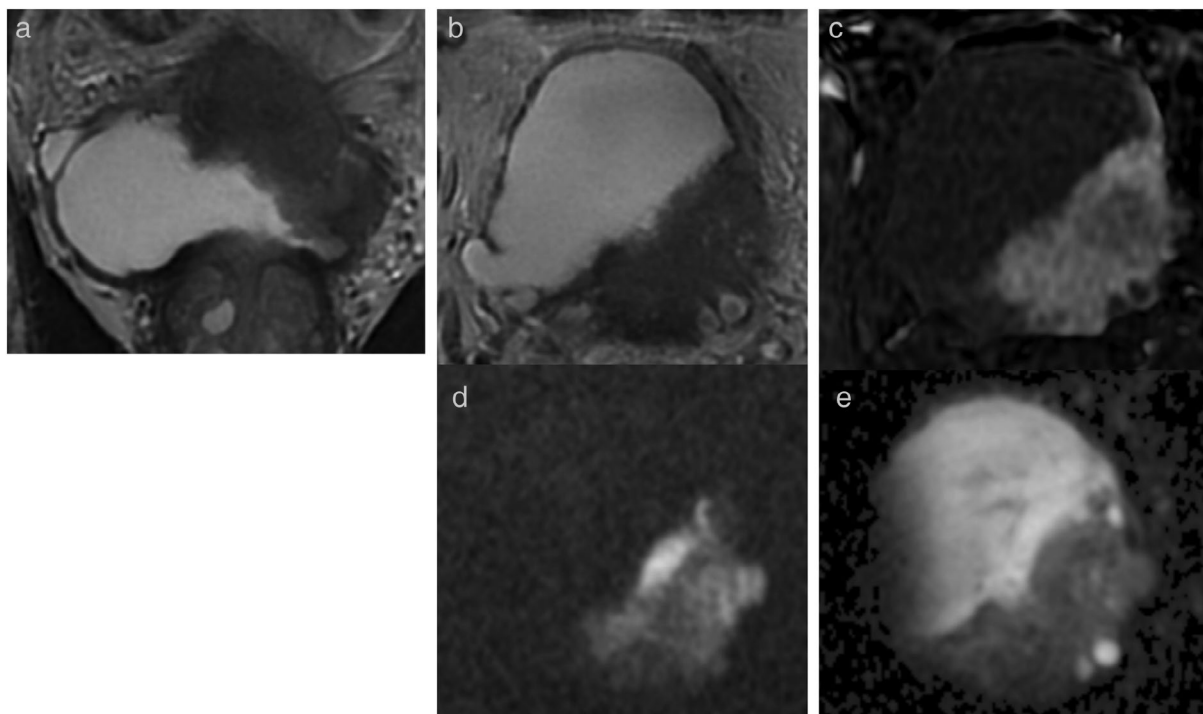


FIGURE 4: A 73-year-old male with positive ultrasound. (a,b) T₂W imaging (coronal, axial plane) shows a sessile mass >1 cm in size at the level of the posterosuperior bladder wall, with intermediate SI that extends through the muscularis propria, invading the perivesical fat tissue. T₂W imaging assigned as VIRADS category 5. (c) DCE imaging shows early and heterogeneous enhancement of the lesion, extending through the muscularis propria, invading the perivesical fat tissue. DCE assigned as VI-RADS category 5. (d,e) DWI (b = 2000) and ADC maps show a lesion with significant restricted diffusion, extending through the muscularis propria, invading the perivesical fat tissue. DWI assigned as VIRADS category 5. Overall VI-RADS score was 5.

respectively (<T2 stage). SC 3 is assigned to exophytic tumor without stalk, or sessile tumor with no clear disruption of low SI muscularis propria, and without a high SI thickened “inner layer.” SC 4 is assigned to tumors associated with an interruption of the low SI muscularis propria still confined to the organ (T2 stage). SC 5 is assigned to tumors extending outside the bladder wall, with invasion of the perivesical fat and/or adjacent organs (≥T3 stage).

ASSESSMENT ON DWI. The single assessment on DW images defines the diffusion weighted category (DW). A bladder mass showing high SI on DWI and low SI on the ADC map extending to the muscularis propria should raise a suspicion of muscle-invasive bladder cancer (≥T2 stage). Tumor stalk and an inner layer have low SI on DWI. DW categories 1 and 2 are assigned to tumors associated with an underlining intermediate SI continuous muscularis propria, smaller or larger than 1 cm, respectively (<T2 stage). DW category 3 is assigned to tumors lacking the descriptors of categories 1 and 2 but corresponding to an SC 2 (on T2W images) and with no clear disruption of low SI muscularis propria. DW categories 4 and 5 are assigned to tumors extending to the muscularis propria (T2 stage) and through the entire bladder wall and beyond (≥T3 stage), respectively.

ASSESSMENT ON DCE. The single assessment on DCE images defines the contrast enhanced category (CE). An enhancing bladder mass associated with early enhancement of the underlining muscularis propria should raise suspicion of muscle-invasive bladder cancer (≥T2 stage). CE category 1 defines tumors corresponding to SC 1, with no early enhancement of the muscularis propria (<T2 stage). CE 2 is assigned to tumors corresponding to SC 2, with no early enhancement of the muscularis propria and with early enhancement of the inner layer (<T2 stage). CE 3 is identical to DW 3. CEs 4 and 5 are assigned to early enhancing tumors extending focally to the muscularis propria (T2 stage) and through the bladder wall and beyond (≥T3 stage), respectively.

A more comprehensive summary of the single categories and overall score is described in Table 2.

Diagnostic Performance

To date, the VI-RADS score has been validated by several research groups, showing good diagnostic performance in detecting muscle-invasive bladder cancer.^{59–72} The first published study investigating the diagnostic accuracy and inter-reader reliability of the VI-RADS score was carried out by Ueno et al⁵⁹ in 2019, on a retrospective cohort of 74 patients. The intraclass correlation coefficients among five readers was

TABLE 2. T-Staging and Final VI-RADS Score According to Single Categories

T-stage	T2WI	DCE	DWI	Final VI-RADS score
T1	Exophytic mass < 1 cm with a continuous underlining detrusor layer (\pm stalk and \pm thickened inner layer) – SC 1	No early enhancement of the detrusor layer – CE 1	Mass hyperintense on DWI and hypointense on ADC map with a continuous underlining detrusor layer on DWI – DW 1	VI-RADS 1
T1	Mass with a continuous underlining detrusor layer (\pm hyperintense thickened inner layer if exophytic or with hyperintense thickened inner layer if sessile) – SC 2	No early enhancement of detrusor layer with early enhancement of inner layer – CE 2	Mass hyperintense on DWI and hypointense on ADC map with a continuous underlining detrusor layer on DWI (with hypointense stalk \pm hypointense thickened inner layer on DWI, if exophytic; with low or intermediate SI thickened inner layer on DWI, if sessile) – DW 2	VI-RADS 2
T1	Disappearance of category 2 findings, but no clear disruption of low SI detrusor layer – SC 3	CE 2	DW 2	VI-RADS 2
T2	Disappearance of category 2 findings, but no clear disruption of low SI detrusor layer – SC 3	Lack of category 2 findings with no clear disruption of hypointense detrusor layer – CE 3	Lack of category 2 findings with no clear disruption of hypointense detrusor layer – DW 3	VI-RADS 3
T2	SC 3	Early enhancing mass that extends focally to detrusor layer – CE 4	High signal-intensity tumor on DWI and low signal-intensity tumor on ADC map extending focally to detrusor layer – DW 4	VI-RADS 4
T2	Extension of the intermediate SI tumor tissue with interruption of low SI line (detrusor layer) – SC 4	CE 4	DW 4	VI-RADS 4
T2	Extension of intermediate SI tumor to extravesical fat, with invasion of the extravesical tissues – SC 5	CE 4	DW 4	VI-RADS 4
>T2	SC 5	Tumor early enhancement extends to the extravesical fat – CE 5	High signal-intensity tumor on DWI and low signal-intensity tumor on ADC map extending to the extravesical fat – DW5	VI-RADS 5

T₂WI = T₂-weighted imaging; DCE = dynamic contrast enhanced; DWI = diffusion weighted imaging; VI-RADS = Vesical Imaging Reporting and Data System; SC = structural category; CE = contrast enhanced category; DW = diffusion weighted category.

0.85 (95% CI, 0.80–0.89) and a pooled AUC was 0.90 (95% CI: 0.87–0.93). Wang et al⁶² in 2019 and Kim et al⁶³ in 2020 published investigations with the two largest retrospective cohorts of patients, respectively 340 and 339. Both groups investigated the sensitivity, specificity, and AUC for VI-RADS scores ≥ 3 ; the results achieved by Wang et al were respectively 87.1% (95% CI: 78–93%), 96.5% (95% CI: 93–98%), and 0.94 (95% CI: 0.90–0.98); the interreader agreement between the two readers was 0.92 (95% CI: 0.85–0.98). Kim et al showed an accuracy of 63.7% (95% CI: 56.4–73.2), sensitivity of 94.6% (95% CI: 90.1–97.9), and specificity of 43.9% (95% CI: 39.5–55.6).

In 2020, Del Giudice et al⁶⁰ published the largest prospective study carried out on a cohort of 231 patients, where the authors showed a good performance of the VI-RADS score in differentiating NMIBC from MIBC, with an accuracy of 0.94 (95% CI: 0.91–0.97); also, as a secondary aim, they examined the possible role of the VI-RADS score to stratify high-risk NMIBC patients as candidates for secondary tumor resection, demonstrating an AUC of 0.93 (95% CI: 0.87–0.97). In March 2020, the first systematic review and meta-analysis was published by Woo et al⁶⁶; it included six studies with a total of 1770 patients included. Pooled sensitivity and specificity were 0.83 (95% CI: 0.70–0.90) and 0.90 (95% CI: 0.83–0.95), and the AUC was 0.94 (95% CI: 0.91–0.95). Factors contributing to heterogeneity among the studies were found to be significantly related to the number of patients in each study, the MRI scan magnetic field strength, the slice thickness of T₂W images, and the VI-RADS cutoff score (≥ 3 vs. ≥ 4). Although pathologic confirmation remains the standard of reference, VI-RADS had proved to be a reliable tool to preoperatively stage BCa, differentiating nonmuscle-invasive from muscle-invasive disease. Table 3 summarizes all published studies investigating the performance of the VI-RADS score.

Discussion

Clinical Implications

To date, the role of MRI in BCa diagnosis and staging has not yet been established.

BCa diagnostic and staging work-up according to European and American guidelines consists mostly of cystoscopy examination and TURBT in patients presenting with hematuria and/or suspicion of BCa after ultrasound exam or positive urinary cytology. Assessment of muscle invasion is essential in staging and treatment of BCa, because therapeutic planning and prognosis are strictly related to it.

In patients with NMIBC, the prognostic risk stratification for recurrence and progression depend on multiple factors: the number of tumors, tumor size, previous recurrence rate, T stage, pathology grade, and the presence of concurrent CIS, according to the EORTC and CUETO models. For

NMIBC, transurethral resection with or without intravesical Bacillus Calmette–Guerin (BCG) instillations is recommended; also, radical cystectomy should be discussed with patients at highest risk of tumor progression.^{73,74} Up to 70% of patients with NMIBC experience disease relapse within 5 years, with 20–30% of patients progressing to muscle-invasive disease despite long-term surveillance after primary therapy.^{75,76} The high rate of recurrence and progression to MIBC are the main factors underlying the high mortality related to BCa. Due to high recurrence rates, often an additional tumor resection (re-TURBT) procedure within 4–6 weeks is required for NMIBC for restaging purposes, in order to avoid understaging.^{10,77–79} Patients with MIBC instead undergo radical cystectomy (when feasible) with or without neoadjuvant chemotherapy (NAC) or immunotherapy for patients enrolled in clinical trials. More than a third of clinically confined tumors show extravesical extension at a final pathologic examination.⁸⁰ Despite improvement in surgical techniques, the rate of relapse remains high, with 5-year survival rates of 36–48% for disease staged $\geq pT3$ -T4 and/or with nodal involvement,⁸¹ with an overall 5-year mortality rate after radical cystectomy ranging from 50–70%.⁸²

Applications of VI-RADS

The use of MRI and the VI-RADS score might fit in multiple settings. Currently, VI-RADS applicability is best suited in the pre-TURBT setting and before intravesical BCG administration. Preoperative MRI and VI-RADS scoring might be used for therapy response prediction by identifying tumors that need initially a more radical approach.⁴² Also, among patients with high-risk NMIBC, VI-RADS scoring might be of use for disease risk stratification and as an indication to undergo secondary resection of the tumor or to avoid it.⁶⁰ However, as previously mentioned, the high tumor recurrence rate and the common need of a secondary tumor resection cannot exclude its use as a follow-up diagnostic modality for disease monitoring. In NMIBC surveillance, MRI might represent a reliable non-invasive alternative to follow-up with cystoscopy, with reduction of disease-related costs. In this setting, structural changes of the bladder wall must be considered. On T₂W images wall thickening, caused by fibrosis and inflammatory changes secondary to the surgical procedure, might be misdiagnosed as BCa recurrence/residue.⁴² To overcome such issues, the application of functional sequences, notably DCE-MRI and DWI, proved to be reliable in differentiating BCa from benign findings.^{36,83,84} In the original VI-RADS document, it was suggested to perform MRI at least 2 weeks after TURBT and BCG administration in order to avoid overstaging caused by posttreatment architectural changes and at least 2 days after cystoscopy or removal of a Foley catheter to lower the risk of artifacts. However, such timing is based on expert consensus and

TABLE 3. Summary of the Published Studies Investigating VI-RADS Performance

First author	Research type, study design	Y. of publ.	No. of patients	Intereader-agreement	Sensitivity (%) (MIBC cutoff)	Specificity (%) (MIBC cutoff)	AUC	Reference standard
Ueno Y, (Japan)	Original Research, <i>R</i>	2019	74	ICC = 0.85	76 (Cat. ≥ 4) 88 (Cat. ≥ 3)	93 (Cat. ≥ 4) 77 (Cat. ≥ 3)	0.90	TUR
Barchetti G, (Italy)	Original Research, <i>R</i>	2019	75	K = 0.731	Reader 1: 91 Reader 2: 82 (Cat. ≥ 3)	Reader 1: 89 Reader 2: 85 (Cat. ≥ 3)	Reader 1: 0.93 Reader 2: 0.87	TUR
Wang H, (China)	Original Research, <i>R</i>	2019	340	K = 0.92	87 (Cat. ≥ 3)	97 (Cat. ≥ 3)	0.94	TUR, PC, RC
Kim SH, (South Korea)	Original Research, <i>R</i>	2019	297	K = 0.89 (T2WI), 0.82 (DWI), 0.85 (DCE)	91 (Cat. ≥ 4) 95 (Cat. ≥ 3)	76 (Cat. ≥ 4) 44 (Cat. ≥ 3)	N/A	TUR, PC, RC
Makboul M, (Egypt)	Original Research, <i>P</i>	2019	50	K = 0.87	78 (Cat. ≥ 3)	88 (Cat. ≥ 3)	0.83	TUR
Del Giudice F, (Italy)	Original Research, <i>P</i>	2019	231	K > 0.92	92 (Cat. ≥ 3)	91 (Cat. ≥ 3)	0.94	TUR, RC
Hong SB, (Korea)	Original Research, <i>R</i>	2020	66	K = 0.97	90 (Cat. ≥ 3)	100 (Cat. ≥ 3)	0.95	TUR, RC
Marchioni M, (Italy)	Original Research, <i>P</i>	2020	38	K = 0.76	86 (Cat. ≥ 4)	87 (Cat. ≥ 4)	0.90	TUR
Liu S, (China)	Original Research, <i>R</i>	2020	126	N/A	94 (Cat. ≥ 4)	92 (Cat. ≥ 4)	0.96	TUR, RC
Wang Z, (China)	Original Research, <i>R</i>	2020	220	N/A	82 (Cat. ≥ 4) 97 (Cat. ≥ 3)	95 (Cat. ≥ 4) 77 (Cat. ≥ 3)	0.96	TUR, PC, RC
Woo S, (USA)	Meta-analysis	2020	1770 (6 studies)	K = 0.81–0.92 ICC = 0.85	83 ^a	90 ^a	0.94 ^a	N/A
Luo C, (China)	Meta-analysis	2020	1064 (6 studies)	N/A	90 ^a	86 ^a	0.93 ^a	N/A

MIBC = muscle invasive bladder cancer; AUC = area under the curve; R = retrospective; P = prospective; TUR = transurethral resection; PC = partial cystectomy, RC = radical cystectomy.
^aPooled measurements.

should be further clarified in future investigations to provide data-driven improvements to the scoring system.

In patients with MIBC, MRI and VI-RADS scoring might be useful to stage tumors likely to benefit from neoadjuvant therapy, to identify tumors suited for bladder-sparing surgery and chemoradiation, and to plan a surgically feasible therapeutic TURBT.^{42,85,86}

Future Perspectives

The VI-RADS score might become a tool for prediction of both tumor aggressiveness and response to therapy, as well as a clinical predictor for perioperative outcomes. Several studies have demonstrated how MRI functional sequences are reliable in determining and predicting tumor aggressiveness.^{46,87–91} Notably, ADC value quantification has been proposed as a potential biomarker by Kobayashi et al, showing that an ADC cutoff value of $0.86 \times 10^{-3} \text{ mm}^2/\text{s}$ (sensitivity of 88%, a specificity of 85%, and an accuracy of 87%) could be used to identify clinically aggressive phenotypes differentiating high grade tumors from less aggressive phenotypes.⁹² A few years before Takeuchi et al proposed the ADC value as a predictor of BCa grading, there were significant differences between the values of G1 and G3 and between G2 and G3.³³

Tumor response to therapy can be evaluated with the use of MRI in different clinical pictures: before, interim, and after therapy. Among others, the role of MRI was assessed by Yoshida et al in 2010 and in 2014, who proposed DWI-MRI as a biomarker to predict chemoradiation sensitivity in MIBC.^{93,94} More recently, Nguyen et al⁹⁵ acquired a data matrix of voxelwise ADC values for each patient before NAC and correlated the results with the patient's response to chemotherapy, demonstrating that resistant tumors were more heterogeneous in their spatial distribution of ADC values. Also, Necchi et al, in 2019, demonstrated the role of MRI in the evaluation of response to therapy before and after immunotherapy, achieving promising results.⁹⁶

MRI application during chemotherapy might stratify patients according to earlier prediction of treatment failure, with the main goal of reducing morbidity and costs. The efficacy of MRI in predicting response was demonstrated by Barentsz et al⁹⁷ in 1998, showing an accuracy, sensitivity, and specificity of 73%, 79%, and 63%, respectively, in distinguishing responders from nonresponders, with T₂WI alone. The results went up to 95%, 93%, and 100%, respectively, when DCE-MRI was evaluated in the analysis. The crucial role of DCE in identification of chemotherapy responders was confirmed later on by other groups, reaching similar results.^{98–100} There is not a large body of evidence investigating the role of MRI in the posttreatment setting. Donaldson et al¹⁰¹ proposed DCE-MRI as a biomarker for evaluation of treatment response after radical cystectomy. Choueiri et al¹⁰² assessed the pathologic response after NAC in patients with MIBC, showing a sensitivity and specificity

of 79% and 55% of DCE-MRI for determining responders, respectively.

Furthermore, MRI and VI-RADS score outcomes have been adopted as clinical predictors of a delayed time to radical interventions (ie, radical cystectomy) in the subpopulation of patients subsequently diagnosed with locally advanced extravesical BCa. In a recently published retrospective cohort series, Del Giudice et al¹⁰³ assessed the diagnostic accuracy of VI-RADS to discriminate interclass features of stage II vs. III BCa. Beyond its high overall accuracy to correlate with pathologically proven $\geq pT3$ tumors (AUC 94.2%, 95% CI: 88.7–99.7), the authors identified VI-RADS score 5 as an independent unfavorable predictor for significant delayed time to cystectomy (ie, >3 months from TURBT diagnosis of MIBC; odds ratio [OR] 2.81, 95% CI: 1.20–6.62). The implication of such preliminary findings might lead in the future to designing clinical trials where VI-RADS could be utilized to minimize the reliance and morbidity of TURBT for MIBC detection and to aid urologists to select the cases that may require urgent radical interventions due to the presence of a high burden of disease.

The body of evidence for the widespread use of MRI in clinical practice is growing; nonetheless, it needs to be reinforced, particularly in the setting of therapy response evaluation and prediction.¹⁰⁴

Limitations and Conclusion

Principal caveats for bladder assessment with MRI are the requirement for an adequate bladder distension, the potential need of an antispasmodic agent injection to reduce motion artifacts, the need to properly define a specific timing and possible imaging pitfalls after TURBT, BCG administration, and neoadjuvant chemo- and immune-therapy in BCa monitoring to avoid overstaging, and the lack of means to evaluate flat urothelial lesions (CIS). Nonetheless, MRI offers significant potential benefits for BCa staging evaluation and most of these limitations can be overcome with the support of future data-driven evidence.

VI-RADS scoring was developed in 2018 by a panel of experts to standardize evaluation and reporting of MRI for BCa staging. It has been proven to be a reliable tool in differentiating nonmuscle-invasive from muscle-invasive bladder cancer. It is also a promising tool in patient stratification for therapeutic planning, disease surveillance, and for the evaluation of tumor aggressiveness and response to therapy. Currently, the widespread use of the score is limited due to narrow expertise and lack of testing. Nonetheless, the VI-RADS score has been consistently validated across several different institutions as an appropriate tool for local staging of BCa and proved to contribute to the diagnostic workup and management of bladder cancer.

Conflict of Interest

All authors declare no conflicts of interest.

Data Availability

Data sharing is not applicable to this article, as no datasets were generated or analyzed during the current study.

References

- Bray F, Ferlay J, Soerjomataram I, Siegel RL, Torre LA, Jemal A. Global cancer statistics 2018: GLOBOCAN estimates of incidence and mortality worldwide for 36 cancers in 185 countries. *CA Cancer J Clin* 2018;68(6):394-424.
- Richters A, Aben KKH, Kiemeny LAML. The global burden of urinary bladder cancer: An update. *World J Urol* 2020;38:1895-1904.
- van Osch FH, Jochems SH, van Schooten F-J, Bryan RT, Zeegers MP. Quantified relations between exposure to tobacco smoking and bladder cancer risk: A meta-analysis of 89 observational studies. *Int J Epidemiol* 2016;45(3):857-870.
- Cassell A, Yunusa B, Jalloh M, et al. Non-muscle invasive bladder cancer: A review of the current trend in Africa. *World J Oncol* 2019;10(3):123-131.
- Al-Husseini MJ, Kunbaz A, Saad AM, et al. Trends in the incidence and mortality of transitional cell carcinoma of the bladder for the last four decades in the USA: A SEER-based analysis. *BMC Cancer* 2019;19(1):46.
- Chamie K, Litwin MS, Bassett JC, et al. Recurrence of high-risk bladder cancer: A population-based analysis: Burden of high-risk bladder cancer. *Cancer* 2013;119(17):3219-3227.
- Morris DS, Weizer AZ, Ye Z, Dunn RL, Montie JE, Hollenbeck BK. Understanding bladder cancer death: Tumor biology versus physician practice. *Cancer* 2009;115(5):1011-1020.
- Mahdavi N, Ghoncheh M, Pakzad R, Momenimovahed Z, Salehiniya H. Epidemiology, incidence and mortality of bladder cancer and their relationship with the development index in the world. *Asian Pac J Cancer Prev* 2016;17(1):381-386.
- Wong MCS, Fung FDH, Leung C, Cheung WWL, Goggins WB, Ng CF. The global epidemiology of bladder cancer: A joinpoint regression analysis of its incidence and mortality trends and projection. *Sci Rep* 2018;8(1):1129.
- Zapała P, Dybowski B, Poletajew S, Białek Ł, Niewczas A, Radziszewski P. Clinical rationale and safety of restaging transurethral resection in indication-stratified patients with high-risk non-muscle-invasive bladder cancer. *World J Surg Oncol* 2018;16(1):6.
- Gomez-Gonzalez JE, Reyes NR. Patterns of global health financing and potential future spending on health. *Lancet* 2017;389(10083):1955-1956.
- Mariotto AB, Robin Yabroff K, Shao Y, Feuer EJ, Brown ML. Projections of the cost of cancer care in the United States: 2010-2020. *J Natl Cancer Inst* 2011;103(2):117-128.
- Mohamed NE, Chaoprang Herrera P, Hudson S, et al. Muscle invasive bladder cancer: Examining survivor burden and unmet needs. *J Urol* 2014;191(1):48-53.
- Lee CT, Mei M, Ashley J, et al. Patient resources available to bladder cancer patients: A pilot study of healthcare providers. *Urology* 2012;79(1):172-177.
- Chung J, Kulkarni GS, Morash R, et al. Assessment of quality of life, information, and supportive care needs in patients with muscle and non-muscle invasive bladder cancer across the illness trajectory. *Support Care Cancer* 2019;27(10):3877-3885.
- Turkbey B, Rosenkrantz AB, Haider MA, et al. Prostate imaging reporting and data system version 2.1: 2019 update of prostate imaging reporting and data system version 2. *Eur Urol* 2019;76(3):340-351.
- Chernyak V, Fowler KJ, Kamaya A, et al. Liver imaging reporting and data system (LI-RADS) version 2018: Imaging of hepatocellular carcinoma in at-risk patients. *Radiology* 2018;289(3):816-830.
- Pavone P, Laghi A, Catalano C, Panebianco V, Fabiano S, Passariello R. MRI of the biliary and pancreatic ducts. *Eur Radiol* 1999;9(8):1513-1522.
- Mann RM, Cho N, Moy L. Breast MRI: State of the art. *Radiology* 2019;292(3):520-536.
- Hickling DR, Sun T-T, Wu X-R. Anatomy and physiology of the urinary tract: Relation to host defense and microbial infection. *Microbiol Spectr* 2015;3(4):1-17.
- Bolla SR, Jetti R. Histology bladder. *StatPearls*. Treasure Island, FL: StatPearls Publishing; 2020. <http://www.ncbi.nlm.nih.gov/books/NBK540963/>.
- Robinson BD, Khani F. Grading, staging, and morphologic risk stratification of bladder cancer. In: Hansel DE, Lerner SP, editors. *Precision Molecular Pathology of Bladder Cancer*. Cham, Switzerland: Springer International Publishing; 2018. p 29-42.
- Bryan RT. Cell adhesion and urothelial bladder cancer: The role of cadherin switching and related phenomena. *Phil Trans R Soc B* 2015;370(1661):20140042.
- Balci MG, Tayfur M. Loss of E-cadherin expression in recurrent non-invasive urothelial carcinoma of the bladder. *Int J Clin Exp Pathol* 2018;11(8):4163-4168.
- Herr H. Preventable cancer deaths associated with bladder preservation for muscle invasive bladder cancer. *Urology* 2019;130:20-21.
- Shen P, Lin M, Hong Y, He X. Bladder preservation approach versus radical cystectomy for high-grade non-muscle-invasive bladder cancer: A meta-analysis of cohort studies. *World J Surg Oncol* 2018;16(1):197.
- Amin MB, American Joint Committee on Cancer, American Cancer Society. *AJCC cancer staging manual*. Eighth edition/editor-in-chief, Amin MB, Edge SB, et al. Chicago: Springer; 2017. p 1024.
- Caglic I, Panebianco V, Vargas HA, et al. MRI of bladder cancer: Local and nodal staging. *J Magn Reson Imaging* 2020;52(3):649-667.
- de Haas RJ, Steyvers MJ, Fütterer JJ. Multiparametric MRI of the bladder: Ready for clinical routine? *Am J Roentgenol* 2014;202(6):1187-1195.
- Lee CH, Tan CH, Faria S de C, Kundra V. Role of imaging in the local staging of urothelial carcinoma of the bladder. *Am J Roentgenol* 2017;208(6):1193-1205.
- Panebianco V, Barchetti F, de Haas RJ, et al. Improving staging in bladder cancer: The increasing role of multiparametric magnetic resonance imaging. *Eur Urol Focus* 2016;2(2):113-121.
- Narumi Y, Kadota T, Inoue E, et al. Bladder tumors: Staging with gadolinium-enhanced oblique MR imaging. *Radiology* 1993;187(1):145-150.
- Takeuchi M, Sasaki S, Ito M, et al. Urinary bladder cancer: Diffusion-weighted MR imaging—Accuracy for diagnosing T stage and estimating histologic grade. *Radiology* 2009;251(1):112-121.
- Hayashi N, Tochigi H, Shiraishi T, Takeda K, Kawamura J. A new staging criterion for bladder carcinoma using gadolinium-enhanced magnetic resonance imaging with an endorectal surface coil: A comparison with ultrasonography. *BJU Int* 2000;85(1):32-36.
- Ma W, Kang SK, Hricak H, Gerst SR, Zhang J. Imaging appearance of granulomatous disease after Intravesical Bacille Calmette-Guérin (BCG) treatment of bladder carcinoma. *Am J Roentgenol* 2009;192(6):1494-1500.
- El-Assmy A, Abou-El-Ghar ME, Refaie HF, Mosbah A, El-Diasty T. Diffusion-weighted magnetic resonance imaging in follow-up of superficial urinary bladder carcinoma after transurethral resection: Initial experience: Diffusion-weighted MRI in bladder cancer follow-up. *BJU Int* 2012;110(11b):E622-E627.

37. Wang H, Pui MH, Guan J, et al. Comparison of early submucosal enhancement and tumor stalk in staging bladder urothelial carcinoma. *Am J Roentgenol* 2016;207(4):797-803.
38. Narumi Y, Kadota T, Inoue E, et al. Bladder wall morphology: in vitro MR imaging—Histopathologic correlation. *Radiology* 1993;187(1): 151-155.
39. Wang H, Pui MH, Guo Y, Yang D, Pan B, Zhou X. Diffusion-weighted MRI in bladder carcinoma: The differentiation between tumor recurrence and benign changes after resection. *Abdom Imaging* 2014;39(1):135-141.
40. Zhou G, Chen X, Zhang J, Zhu J, Zong G, Wang Z. Contrast-enhanced dynamic and diffusion-weighted MR imaging at 3.0T to assess aggressiveness of bladder cancer. *Eur J Radiol* 2014;83(11):2013-2018.
41. Panebianco V, De Berardinis E, Barchetti G, et al. An evaluation of morphological and functional multi-parametric MRI sequences in classifying non-muscle and muscle invasive bladder cancer. *Eur Radiol* 2017;27(9):3759-3766.
42. Panebianco V, Narumi Y, Altun E, et al. Multiparametric magnetic resonance imaging for bladder cancer: Development of VI-RADS (vesical imaging-reporting and data system). *Eur Urol* 2018;74(3):294-306.
43. Yu RJ, Stein JP, Cai J, Miranda G, Groshen S, Skinner DG. Superficial (pT2a) and deep (pT2b) muscle invasion in pathological staging of bladder cancer following radical cystectomy. *J Urol* 2006;176(2): 493-499.
44. Magers MJ, Lopez-Beltran A, Montironi R, Williamson SR, Kaimakliotis HZ, Cheng L. Staging of bladder cancer. *Histopathology* 2019;74(1):112-134.
45. Alfred Witjes J, Lebrecht T, Comp erat EM, et al. Updated 2016 EAU guidelines on muscle-invasive and metastatic bladder cancer. *Eur Urol* 2017;71(3):462-475.
46. Takeuchi M, Sasaki S, Naiki T, et al. MR imaging of urinary bladder cancer for T-staging: A review and a pictorial essay of diffusion-weighted imaging: DWI of urinary bladder cancer staging. *J Magn Reson Imaging* 2013;38(6):1299-1309.
47. Sureka B, Kumar M, Malik A, Bhushan T, Mohanty N, Gupta N. Comparison of dynamic contrast-enhanced and diffusion weighted magnetic resonance image in staging and grading of carcinoma bladder with histopathological correlation. *Urol Ann* 2015;7(2):199-204.
48. Gandhi N, Krishna S, Booth CM, et al. Diagnostic accuracy of magnetic resonance imaging for tumour staging of bladder cancer: Systematic review and meta-analysis. *BJU Int* 2018;122(5):744-753.
49. Woo S, Suh CH, Kim SY, Cho JY, Kim SH. Diagnostic performance of MRI for prediction of muscle-invasiveness of bladder cancer: A systematic review and meta-analysis. *Eur J Radiol* 2017;95:46-55.
50. Huang L, Kong Q, Liu Z, Wang J, Kang Z, Zhu Y. The diagnostic value of MR imaging in differentiating T staging of bladder cancer: A meta-analysis. *Radiology* 2018;286(2):502-511.
51. Zhang N, Wang X, Wang C, et al. Diagnostic accuracy of multiparametric magnetic resonance imaging for tumor staging of bladder cancer: Meta-analysis. *Front Oncol* 2019;9:981.
52. Kim H, Lim JS, Choi JY, et al. Rectal cancer: Comparison of accuracy of local-regional staging with two- and three-dimensional preoperative 3-T MR imaging. *Radiology* 2010;254(2):485-492.
53. Caglic I, Povalej Brzan P, Warren AY, Bratt O, Shah N, Barrett T. Defining the incremental value of 3D T2-weighted imaging in the assessment of prostate cancer extracapsular extension. *Eur Radiol* 2019;29(10):5488-5497.
54. Valerio M, Zini C, Fierro D, et al. 3T multiparametric MRI of the prostate: Does intravoxel incoherent motion diffusion imaging have a role in the detection and stratification of prostate cancer in the peripheral zone? *Eur J Radiol* 2016;85(4):790-794.
55. Engels RRM, Isra el B, Padhani AR, Barentsz JO. Multiparametric magnetic resonance imaging for the detection of clinically significant prostate cancer: What urologists need to know. Part 1: Acquisition. *Eur Urol* 2019;77(4):457-468.
56. Warndahl BA, Borisch EA, Kawashima A, Riederer SJ, Froemming AT. Conventional vs. reduced field of view diffusion weighted imaging of the prostate: Comparison of image quality, correlation with histology, and inter-reader agreement. *Magn Reson Imaging* 2018;47:67-76.
57. Paner GP, Montironi R, Amin MB. Challenges in pathologic staging of bladder cancer: Proposals for fresh approaches of assessing pathologic stage in light of recent studies and observations pertaining to bladder histoanatomic variances. *Adv Anat Pathol* 2017;24(3): 113-127.
58. Xiao G-Q, Rashid H. Bladder neck urothelial carcinoma: A urinary bladder subsite carcinoma with distinct clinicopathology. *Int J Surg Pathol* 2015;23(7):517-523.
59. Ueno Y, Takeuchi M, Tamada T, et al. Diagnostic accuracy and inter-observer agreement for the vesical imaging-reporting and data system for muscle-invasive bladder cancer: A multireader validation study. *Eur Urol* 2019;76(1):54-56.
60. Del Giudice F, Barchetti G, De Berardinis E, et al. Prospective assessment of vesical imaging reporting and data system (VI-RADS) and its clinical impact on the management of high-risk non-muscle-invasive bladder cancer patients candidate for repeated transurethral resection. *Eur Urol* 2020;77(1):101-109.
61. Barchetti G, Simone G, Ceravolo I, et al. Multiparametric MRI of the bladder: Inter-observer agreement and accuracy with the vesical imaging-reporting and data system (VI-RADS) at a single reference center. *Eur Radiol* 2019;29(10):5498-5506.
62. Wang H, Luo C, Zhang F, et al. Multiparametric MRI for bladder cancer: Validation of VI-RADS for the detection of detrusor muscle invasion. *Radiology* 2019;291(3):668-674.
63. Kim SH. Validation of vesical imaging reporting and data system for assessing muscle invasion in bladder tumor. *Abdom Radiol* 2019;45(2): 491-498.
64. Makboul M, Farghaly S, Abdelkawi IF. Multiparametric MRI in differentiation between muscle invasive and non-muscle invasive urinary bladder cancer with vesical imaging reporting and data system (VI-RADS) application. *BJR* 2019;92(1104):20190401.
65. Hong SB, Lee NK, Kim S, et al. Vesical imaging-reporting and data system for multiparametric MRI to predict the presence of muscle invasion for bladder cancer: Accuracy of VI-RADS in bladder cancer. *J Magn Reson Imaging* 2020.
66. Woo S, Panebianco V, Narumi Y, et al. Diagnostic performance of vesical imaging reporting and data system for the prediction of muscle-invasive bladder cancer: A systematic review and meta-analysis. *Eur Urol Oncol* 2020;3(3):306-315.
67. Luo C, Huang B, Wu Y, Chen J, Chen L. Use of vesical imaging-reporting and data system (VI-RADS) for detecting the muscle invasion of bladder cancer: A diagnostic meta-analysis. *Eur Radiol* 2020;30(8): 4606-4614.
68. Pecoraro M, Takeuchi M, Vargas HA, et al. Overview of VI-RADS in bladder cancer. *Am J Roentgenol* 2020;214(6):1259-1268.
69. Hechler V, Rink M, Beyersdorff D, et al. Bedeutung der VI-RADS-Klassifikation f ur die Bildgebung beim Harnblasenkarzinom – Stand der Dinge. *Urologe* 2019;58(12):1443-1450.
70. Wang Z, Shang Y, Luan T, et al. Evaluation of the value of the VI-RADS scoring system in assessing muscle infiltration by bladder cancer. *Cancer Imaging* 2020;20(1):26.
71. Marchioni M, Primiceri G, Delli Pizzi A, et al. Could bladder multiparametric MRI be introduced in routine clinical practice? Role of the new VI-RADS score: Results from a prospective study. *Clin Genitourin Cancer* 2020; epub ahead of print.
72. Liu S, Xu F, Xu T, Yan Y, Yao X, Tang G. Evaluation of vesical imaging-reporting and data system (VI-RADS) scoring system in predicting muscle invasion of bladder cancer. *Transl Androl Urol* 2020;9(2):445-451.
73. Babjuk M, Burger M, Comp erat EM, et al. European Association of Urology guidelines on non-muscle-invasive bladder cancer (TaT1 and carcinoma in situ) — 2019 update. *Eur Urol* 2019;76(5):639-657.

74. <https://www.auanet.org/guidelines/bladder-cancer-non-muscle-invasive-guideline#x3701>. 202AD.
75. Zhu C-Z, Ting H-N, Ng K-H, Ong T-A. A review on the accuracy of bladder cancer detection methods. *J Cancer* 2019;10(17):4038-4044.
76. Aldousari S, Kassouf W. Update on the management of non-muscle invasive bladder cancer. *Can Urol Assoc J* 2010;4(1):56-64.
77. Brausi M, Collette L, Kurth K, van der Meijden AP, et al. Variability in the recurrence rate at first follow-up cystoscopy after TUR in stage ta T1 transitional cell carcinoma of the bladder: A combined analysis of seven EORTC studies. *Eur Urol* 2002;41(5):523-531.
78. Richterstetter M, Wullich B, Amann K, et al. The value of extended transurethral resection of bladder tumour (TURBT) in the treatment of bladder cancer: Value of extended turbt for treating bladder cancer. *BJU Int* 2012;110(2b):E76-E79.
79. Herr HW, Donat SM. Quality control in transurethral resection of bladder tumours. *BJU Int* 2008;102(9b):1242-1246.
80. Shariat SF, Palapattu GS, Karakiewicz PI, et al. Discrepancy between clinical and pathologic stage: Impact on prognosis after radical cystectomy. *Eur Urol* 2007;51(1):137-151.
81. Hautmann RE, Gschwend JE, de Petriconi RC, Kron M, Volkmer BG. Cystectomy for transitional cell carcinoma of the bladder: Results of a surgery only series in the neobladder era. *J Urol* 2006;176(2):486-492.
82. Park JC, Citrin DE, Agarwal PK, Apolo AB. Multimodal management of muscle-invasive bladder cancer. *Curr Probl Cancer* 2014;38(3):80-108.
83. Barentsz JO, Jager GJ, van Vierzen PB, et al. Staging urinary bladder cancer after transurethral biopsy: Value of fast dynamic contrast-enhanced MR imaging. *Radiology* 1996;201(1):185-193.
84. Johnson RJ, Carrington BM, Jenkins JPR, Barnard RJ, Read G, Isherwood I. Accuracy in staging carcinoma of the bladder by magnetic resonance imaging. *Clin Radiol* 1990;41(4):258-263.
85. Seisen T, Sun M, Lipsitz SR, et al. Comparative effectiveness of trimodal therapy versus radical cystectomy for localized muscle-invasive urothelial carcinoma of the bladder. *Eur Urol* 2017;72(4):483-487.
86. International Collaboration of Trialists on behalf of the Medical Research Council Advanced Bladder Cancer Working Party (now the National Cancer Research Institute Bladder Cancer Clinical Studies Group), the European Organisation for Research and Treatment of Cancer Genito-Urinary Tract Cancer Group, the Australian Bladder Cancer Study Group, the National Cancer Institute of Canada Clinical Trials Group, Finnbladder, Norwegian Bladder Cancer Study Group, and Club Urologico Espanol de Tratamiento Oncologic. International phase III trial assessing neoadjuvant cisplatin, methotrexate, and vinblastine chemotherapy for muscle-invasive bladder cancer: Long-term results of the BA06 30894 trial. *JCO* 2011;29(16):2171-2177.
87. Yoshida S, Takahara T, Kwee TC, Waseda Y, Kobayashi S, Fujii Y. DWI as an imaging biomarker for bladder cancer. *Am J Roentgenol* 2017;208(6):1218-1228.
88. Kikuchi K, Shigihara T, Hashimoto Y, et al. Apparent diffusion coefficient on magnetic resonance imaging (MRI) in bladder cancer: Relations with recurrence/progression risk. *FJMS* 2017;63(2):90-99.
89. Abdelsalam EM, EL Adalany MA, Fouda MEA. Value of diffusion weighted magnetic resonance imaging in grading of urinary bladder carcinoma. *Egypt J Radiol Nucl Med* 2018;49(2):509-518.
90. Yamada Y, Kobayashi S, Isoshima S, Arima K, Sakuma H, Sugimura Y. The usefulness of diffusion-weighted magnetic resonance imaging in bladder cancer staging and functional analysis. *J Can Res Ther* 2014;10(4):878-882.
91. Matsuki M, Inada Y, Tatsugami F, Tanikake M, Narabayashi I, Katsuoka Y. Diffusion-weighted MR imaging for urinary bladder carcinoma: Initial results. *Eur Radiol* 2007;17(1):201-204.
92. Kobayashi S, Koga F, Yoshida S, et al. Diagnostic performance of diffusion-weighted magnetic resonance imaging in bladder cancer: Potential utility of apparent diffusion coefficient values as a biomarker to predict clinical aggressiveness. *Eur Radiol* 2011;21(10):2178-2186.
93. Yoshida S. Diffusion-weighted magnetic resonance imaging in management of bladder cancer, particularly with multimodal bladder-sparing strategy. *WJR* 2014;6(6):344-354.
94. Yoshida S, Koga F, Kawakami S, et al. Initial experience of diffusion-weighted magnetic resonance imaging to assess therapeutic response to induction chemoradiotherapy against muscle-invasive bladder cancer. *Urology* 2010;75(2):387-391.
95. Nguyen HT, Mortazavi A, Pohar KS, et al. Quantitative assessment of heterogeneity in bladder tumor MRI diffusivity: Can response be predicted prior to neoadjuvant chemotherapy? *BLC* 2017;3(4):237-244.
96. Necchi A, Bandini M, Calareso G, et al. Multiparametric magnetic resonance imaging as a noninvasive assessment of tumor response to neoadjuvant pembrolizumab in muscle-invasive bladder cancer: Preliminary findings from the PURE-01 study. *Eur Urol* 2019;77(5):636-643.
97. Barentsz JO, Berger-Hartog O, Witjes JA, et al. Evaluation of chemotherapy in advanced urinary bladder cancer with fast dynamic contrast-enhanced MR imaging. *Radiology* 1998;207(3):791-797.
98. Chakiba C, Cornelis F, Descat E, et al. Dynamic contrast enhanced MRI-derived parameters are potential biomarkers of therapeutic response in bladder carcinoma. *Eur J Radiol* 2015;84(6):1023-1028.
99. Schrier BP, Peters M, Barentsz JO, Witjes JA. Evaluation of chemotherapy with magnetic resonance imaging in patients with regionally metastatic or unresectable bladder cancer. *Eur Urol* 2006;49(4):698-703.
100. Nguyen HT, Jia G, Shah ZK, et al. Prediction of chemotherapeutic response in bladder cancer using K-means clustering of dynamic contrast-enhanced (DCE)-MRI pharmacokinetic parameters: Chemotherapeutic response in bladder cancer. *J Magn Reson Imaging* 2015;41(5):1374-1382.
101. Donaldson SB, Bonington SC, Kershaw LE, et al. Dynamic contrast-enhanced MRI in patients with muscle-invasive transitional cell carcinoma of the bladder can distinguish between residual tumour and post-chemotherapy effect. *Eur J Radiol* 2013;82(12):2161-2168.
102. Choueiri TK, Jacobus S, Bellmunt J, et al. Neoadjuvant dose-dense methotrexate, vinblastine, doxorubicin, and cisplatin with pegfilgrastim support in muscle-invasive urothelial cancer: Pathologic, radiologic, and biomarker correlates. *JCO* 2014;32(18):1889-1894.
103. Del Giudice F, Leonardo C, Simone G, et al. Preoperative detection of VI-RADS (vesical imaging-reporting and data system) score 5 reliably identifies extravesical extension of urothelial carcinoma of the urinary bladder and predicts significant delayed time-to-cystectomy: Time to reconsider the need. *BJU Int* 2020. epub ahead of print.
104. O'Connor JPB, Aboagye EO, Adams JE, et al. Imaging biomarker roadmap for cancer studies. *Nat Rev Clin Oncol* 2017;14(3):169-186.